Supporting Information

Rinnerthaler et al. 10.1073/pnas.1201629109

SI Results

Specific Activity of Yno1p. Yeast WT cells transformed either with the empty plasmid pYES2 or with pYES2-*YNO1* and grown with galactose as carbon source to induce expression of the insert were broken up as described in *SI Materials and Methods*. Microsomes were prepared and reactive oxygen species (ROS) production and protein content were determined in the 2,000 × *g* supernatant and in the purified microsome fraction (100,000 × *g* pellet). The increase in specific activity (ROS production/micrograms of protein) comparing the two fractions was 4.49-fold for WT cells without overexpression of Yno1p, and 1.86-fold for WT cells overexpressing Yno1p. Experiments were done three times with very similar results. The smaller purification factor for the overexpression strain is due to its larger Yno1 protein content in the microsomes.

SI Materials and Methods

Phylogenetic Tree. The phylogenetic tree was built with 94 full-length sequences of known NADPH oxidases and ferric reductases, on the basis of the nearest neighbor joining method (1) with the program AlignX as part of the Vector NTI Advance10 Suite (Invitrogen). The tree was displayed with the Interactive Tree Of Life (http://itol.embl.de/index.shtml).

Determination of Free Iron. The free iron concentration was measured according to ref. 2. Briefly, 70 μL of the cleared cell lysate was mixed with 100 μL 1 M Tris-HCl pH 7.4, 60 μL 10% (wt/vol) SDS, 20 μL 1 M sodium dithionite, 100 μL of 100 mM bathophenantroline, and 650 μL H_2O. The mixture was incubated for 5 min at 20 °C and pelleted for 5 min at 10,000 × *g*. The absorption spectra of the supernatant was then measured between 500 and 700 nm, with an absorption peak at 540 nm, representing the measured Fe^{2+}-bathophenantroline complex. A calibration curve was obtained using appropriate $FeSO_4$ concentrations.

Determination of Total Iron by Atomic Absorption Spectrometry. Total iron concentration was determined by graphite furnace atomic absorption spectrophotometry using an instrument (Perkin-Elmer; 5000 Zeeman) equipped with an electrothermal atomization unit (HGA-500) and an automatic sample injector (AS-40). The absorption at 248.3 nm (0.2 nm, low slit) from an iron hollow cathode lamp was measured. A total of 20 μL of sample was injected in a pyrolytical graphite tube. The area under the atomization signal peak was integrated by the instrument. All final samples contained 0.01 M HNO_3 to prevent the absorption of trace metal onto the cup wall.

DNA Manipulations and Cloning Techniques. All genes were first cloned into the mammalian expression vector pcDNA3.1/HYGRO(−) (Invitrogen), then subcloned into different plasmids.

The following yeast shuttle vectors were used in this study: For GFP fusions the centromeric vector pUG35 was used (3). For overexpression experiments the galactose-inducible plasmid pYES2 (Invitrogen) and the doxycycline-inducible vector pCM297 (4) were used.

PCR products were amplified with the KOD polymerase (Novagen). Restriction enzymes were obtained from Fermentas. All constructs were sequenced at Eurofins MWG Operon. The inserts *FRE1*, *FRE4*, and YGL160W were subcloned from the plasmid pCDNA3.1/HYGRO(−) into the vector pCM297 with PmeI. *FRE8* was cloned from pGEM-T into plasmid pCDNA3.1/HYGRO(−) and pCM297 with NotI. pCDNA3.1/HYGRO(−)–*FRE3* was cut with KpnI, the sticky end was blunted with the Klenow polymerase, then cut with BamHI and cloned into the vector pCM297 linearized with BamHI and HpaI. FRE7 was cut out from the plasmid pCDN3.1/HYGRO(−) and cloned into the vector pCM297 with EcoRI. The ORF YGL160W was cut out from pCM297 and cloned into pYES2 with BamHI. *FRE1* was excised from pCDNA3.1/HYGRO(−) with SacI and cloned into the vector pYES2. *PaNOX1* and *PaNOX2* were cut out from the vector pFL61 with NotI and cloned into pCM297. *PaNOX1* was subcloned from pCM297 to vector pYES2 with NotI.

SI Spot Tests

The sensitivity or resistance of a *YNO1* deletion strain was tested by spotting yeast cells on SC −glucose plates containing various concentrations of oxidants, the reductant dithiothreitol (DTT) or wiskostatin: menadione (0.05–0.35 mM), diamide(1–2 mM), *tert*-butyl hydrogen peroxide (0.8–2 mM), H_2O_2 (1–5 mM), wiskostatin (10–50 μM), and DTT (10–50 mM). Both WT and Δ*yno1* strains were grown to stationary phase in liquid SC −glucose and were then diluted to the following OD_{600} values: 3.0, 1.0, 0.3, and 0.1. Ten-microliter aliquots were spotted onto the appropriate plates. The strains were incubated for 3 d at 28 °C.

Electron Microscopy. Sediments were dissolved in 10 μL of appropriate buffer. Five-microliter drops were applied onto glow-discharge–activated (5) formvar/carbon grids and let to adsorb for 30 s. After that, the grids were negatively stained with 2% (wt/vol) uranyl acetate. Samples were viewed in Philips CM100 electron microscope at 80 kV. Digital images were recorded using a slow-scan MegaViewII camera.

Protein Determination. Microsomal pellet was resuspended in 250 mM sucrose, 50 mM Tris pH 4.5, 22 mg/mL octyl-β-D-glucopyranoside (Sigma) were added, incubated for 10 min, and 20 μL of this solution was added to 1 mL of Bradford reagent (Pierce), incubated for 5 min in the dark, and absorbance at 595 nm was measured. Calibration curve was prepared with bovine serum albumine.

Preparation of Yeast Microsomes. A total of 4×10^9 cells of each strain to be tested were pelleted at 1,000 × *g* for 3 min at 4 °C and resuspended in 10 mL 250 mM sucrose, 50 mM Tris-HCl, pH 4.5. Three mL of glass beads (0.25 to 0.5 mm diameter; Merck) were added and the cells were broken in a bead beater (FastPrep-24; MP Biomedical) and transferred to precooled Sorvall SS34 centrifuge tubes and cetrifuged at 2,000 × *g* for 10 min to remove unbroken cells and cell walls. The supernatant was centrifuged at 18,500 × *g* for 10 min at 4 °C to pellet mitochondria. The supernatant was centrifuged at 100,000 × *g* for 2 h in a Sorvall Ultra Pro-80 centrifuge (TH-641 swing-out rotor) and the pellet containing the microsomal fraction (see also electron microscopy) was resuspended in 1 mL 250 mM sucrose, 50 mM Tris-HCl, pH 4.5.

ROS Measurements of Microsomal Fractions. Ninety microliters of the microsomal fraction was mixed with 90 μL of a 10 μg/mL dihydroethidium (DHE) solution in a black microwell plate (Nunc). Appropriate coenzymes and/or inhibitors were added and after a 15-min incubation in the dark at 28 °C the fluorescence was measured in an Anthos Zenyth 3100 (Anthos Labtec Instruments) plate reader with an excitation wavelength of 485 nm and an emission wavelength of 595 nm. Depending on the experiment, 200 μM NADPH or 100 μM NADH was added. To

test inhibition of the NADPH oxidase activity of Yno1p, the microsomal fraction was preincubated with 100 μM diphenyleneiodonium chloride (DPI); Sigma) for 30 min after which treatment NADPH was added.

Endoplasmic Reticulum (ER) Stress. ER stress was induced by the addition of tunicamycin (Sigma) to a final concentration of 10 μg/mL (stock: 1 mg/mL in DMSO) and incubation for 8 h at 37 °C under constant agitation.

Statistical Analysis. Data are reported as mean values of at least three independent determinations and presented as mean ± SD. Statistical analyses were performed using the two-tailed Student *t* test. Significant difference at the *95, **99, and ***99.9% levels.

1. Saitou N, Nei M (1987) The neighbor-joining method: A new method for reconstructing phylogenetic trees. *Mol Biol Evol* 4:406–425.
2. Molik S, Lill R, Mühlenhoff U (2007) Methods for studying iron metabolism in yeast mitochondria. *Methods Cell Biol* 80:261–280.
3. Hegemann JH, et al. (1999) A fast method to diagnose chromosome and plasmid loss in Saccharomyces cerevisiae strains. *Yeast* 15(10B):1009–1019.
4. Klinger H, et al. (2010) Quantitation of (a)symmetric inheritance of functional and of oxidatively damaged mitochondrial aconitase in the cell division of old yeast mother cells. *Exp Gerontol* 45:533–542.
5. Benada O, Pokorný V (1990) Modification of the Polaron sputter-coater unit for glow-discharge activation of carbon support films. *J Electron Microsc Tech* 16:235–239.

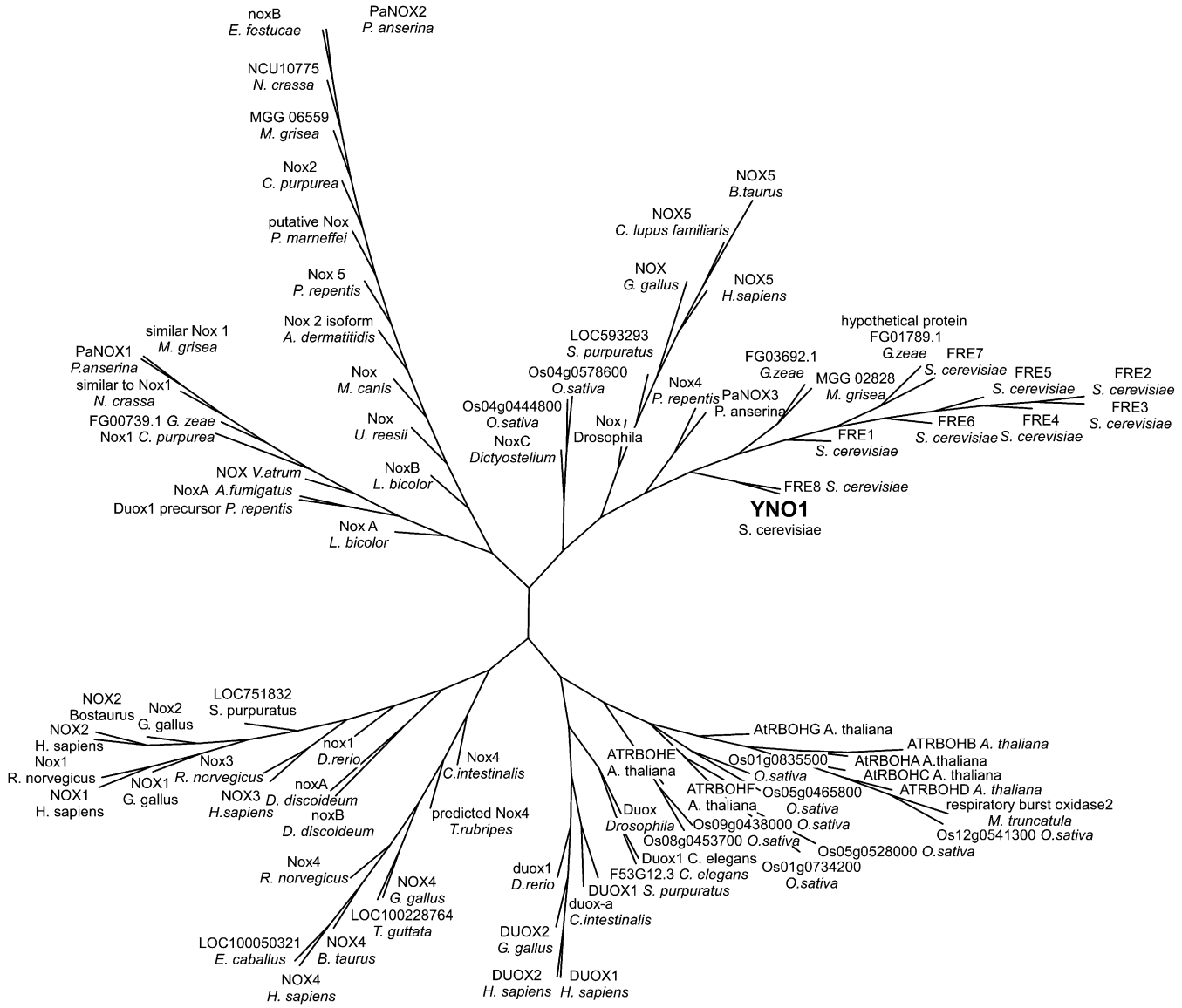

Fig. S1. Phylogenetic tree of NOX enzymes and ferric reductases. Among the nine homologs of this protein superfamily, *FRE1–FRE7* are grouped as very close neighbors, whereas *FRE8* and *YNO1* together cluster at a different location. The closest homolog to *YNO1* is *FRE8*, which is not a ferric reductase (1). Among the fungal members of this protein superfamily, *YNO1* is most closely related to fungal NOXC, and the closest relationship to mammalian NADPH oxidases is to NOX5.

1. De Freitas JM, Liba A, Meneghini R, Valentine JS, Gralla EB (2000) Yeast lacking Cu-Zn superoxide dismutase show altered iron homeostasis. Role of oxidative stress in iron metabolism. *J Biol Chem* 275:11645–11649.

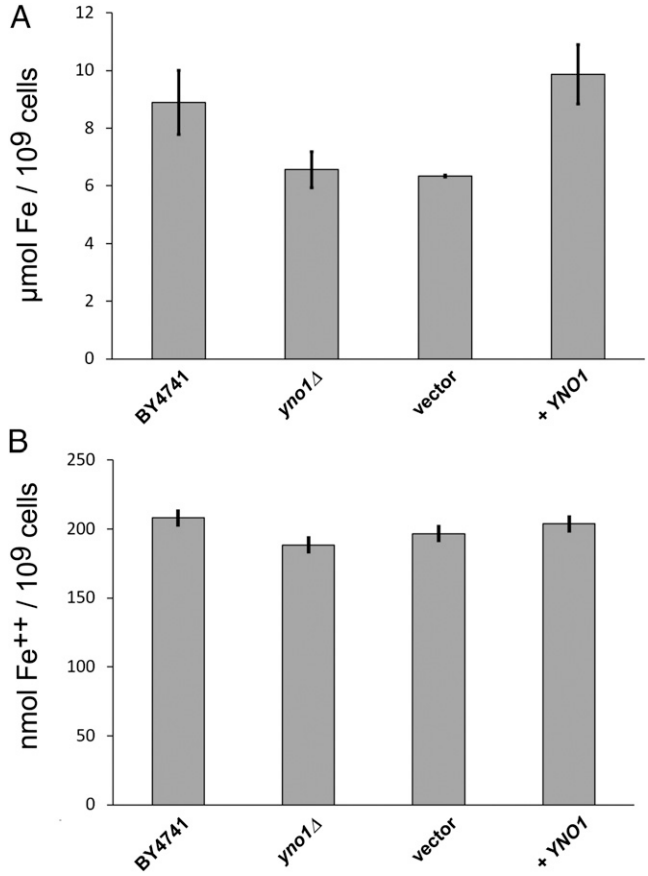

Fig. S2. Iron measurements. (*A*) Total iron measurement with atomic absorption spectroscopy. Total iron concentrations were slightly but not significantly increased when the *YNO1* overexpressing strain was compared with the BY4741 WT strain. (*B*) Measurement of free ferrous iron with bathophenantroline. No significant difference between all four measured cultures could be detected.

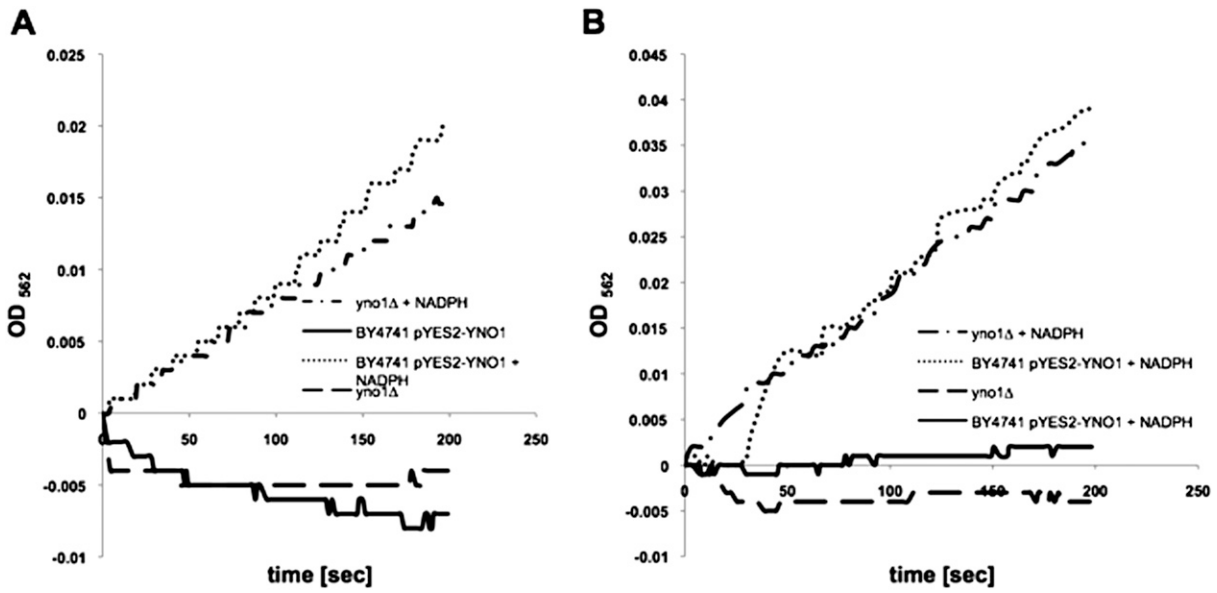

Fig. S3. Determination of ferric reductase activity in yeast microsomes. Two independent experiments are shown measuring ferric reductase activities of microsomes of a strain overexpressing *YNO1* or being deleted for *YNO1*. Conditions were exactly as described by ref. 1 using the buffer described and titrated to pH 6.0. Absorption was normalized by subtraction of blanks. *Upper* curves in each experiment were obtained with the overexpression strain and the deletion strain, respectively, and are very similar, indicating that the small change in arbitrary units over the course of a few minutes is due to a background activity of the microsomes, not to Yno1p. The values obtained were 0.01 and 0.02 arb. units/min. The specific activity of the background ferric reductase was 16 nmol/min × mg protein in experiment A and 27 nmol/min × mg protein in experiment B. *Lower* curves were obtained by leaving out NADPH, showing that the small background activity does depend on NADPH.

1. Wyman S, Simpson RJ, McKie AT, Sharp PA (2008) Dcytb (Cybrd1) functions as both a ferric and a cupric reductase in vitro. *FEBS Lett* 582:1901–1906.

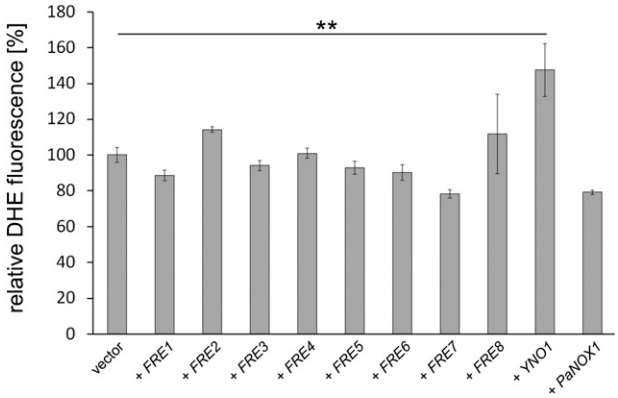

Fig. S4. DHE measurements of the nine members of the NOX/IMR protein family in *Saccharomyces cerevisiae*. All seven putative ferric reductases (*FRE1–FRE7*), *YNO1*, *FRE8*, and *PaNOX1* were cloned into the expression vector pCM297 (4). Expression was induced by the addition of 100 mg/L doxycyline. Only the Yno1p overexpressing strain showed an approximately 50% increase in superoxide levels.

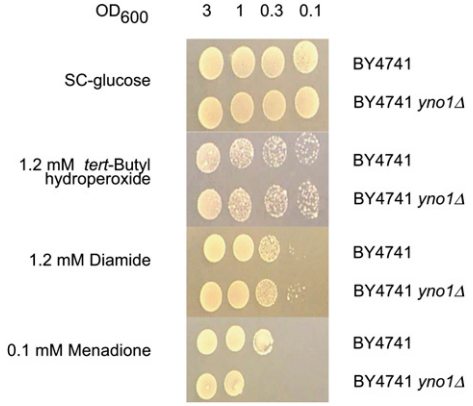

Fig. S5. Wild-type cells and cells deleted for *YNO1* were spotted onto plates containing either *tert*-butylhydroperoxide, diamide, or menadione. The *yno1*Δ deletion mutant was slightly sensitive to menadione, whereas on plates containing *tert*-butyl-hydroperoxide or diamide no difference in growth was observed.

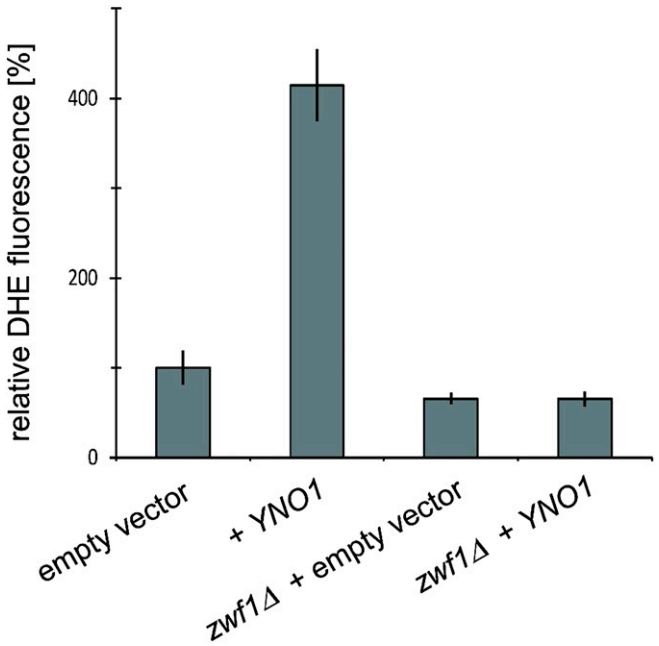

Fig. S6. ROS measurements by DHE fluorescence in the BY4741 background testing the influence of the *zwf1* deletion. Deletion of *zwf1* allows normal growth in the absence of stress. Overexpression of *YNO1* in a *zwf1Δ* strain did not lead to an increase in ROS levels compared with controls, showing that intracellular NADPH is required for ROS production through Yno1p.

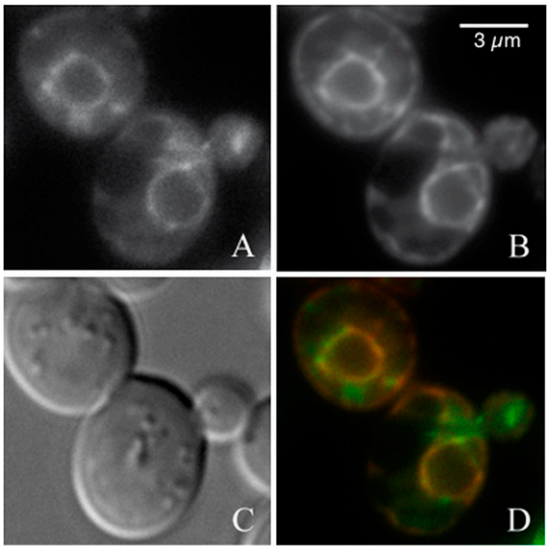

Fig. S7. Two budded yeast cells expressing YNO1-GFP as well as HDEL-RFP (1) were analyzed by fluorescence microscopy as described in *Materials and Methods*. (*A*) YNO1–eGFP stain, (*B*) HDEL-RFP stain, (*C*) phase contrast, and (*D*) overlay of *A*–*C*. Colocalization of both fluorescent markers in the perinuclear ER can be seen. A small part of the YNO1–eGFP is located in the cytoplasm.

1. Friedman JR, et al. (2011) ER tubules mark sites of mitochondrial division. *Science* 334:358–362.

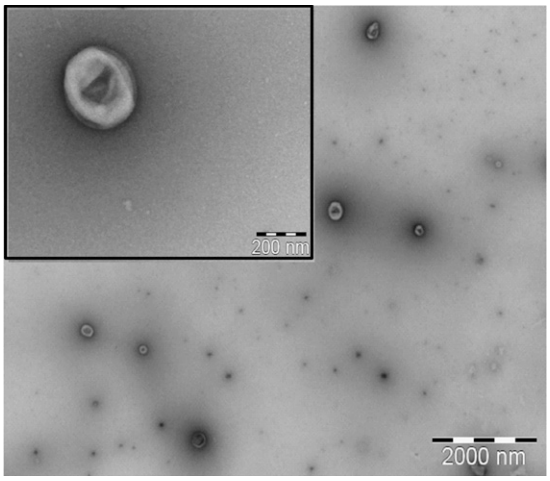

Fig. S8. Transmission electron microscopy of the osmotically stabilized microsomal fraction was performed as described in *SI Materials and Methods*. Microsomes appeared as closed membrane vesicles with diameters between 50 and 200 nm.

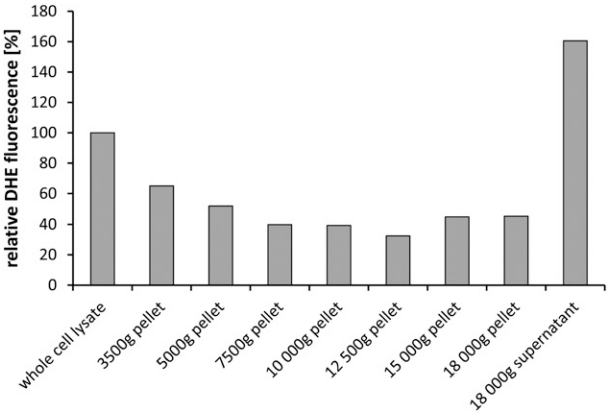

Fig. S9. Cell fractions obtained by differential centrifugation were tested for ROS production after addition of 200 μM NADPH. An increased level in DHE oxidation could only be detected in the microsome-containing 18,000 × *g* supernatant, confirming the results of the ER localization of Yno1p–eGFP. The cells were broken with glass beads in 250 mM sucrose, 50 mM Tris-HCl, pH 4.5, all fractions (pellets were resuspended in 250 mM sucrose, 50 mM Tris-HCl, pH 4.5) were adjusted to equal volumes before ROS measurements.

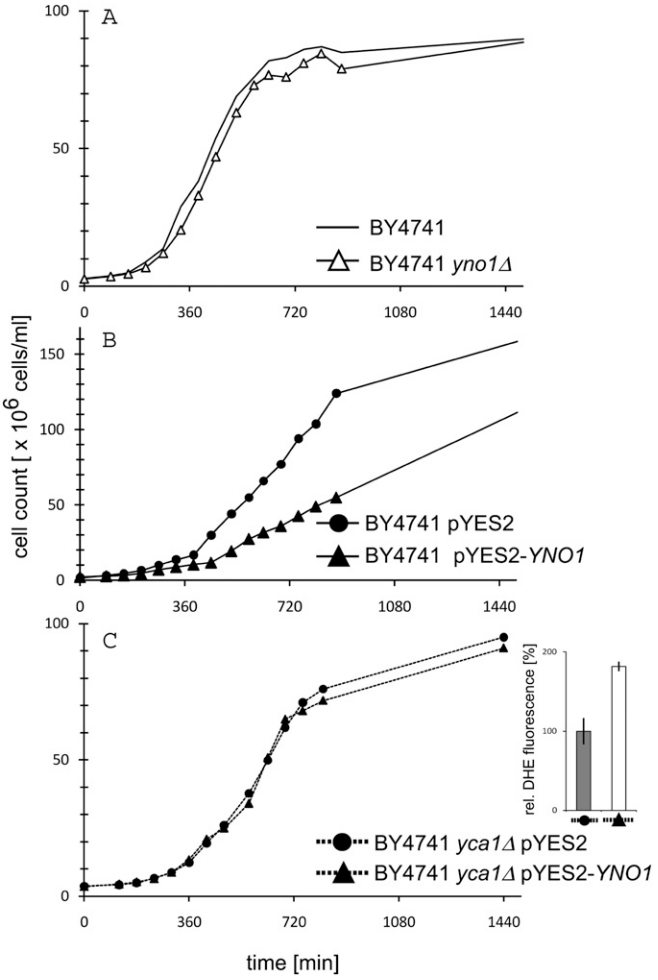

Fig. S10. Growth curves of WT, *yno1Δ*, and *yca1Δ* strains overexpressing YNO1 under galactose control or in the absence of *YNO1* overexpression (vector control). (*A*) WT and *yno1Δ* strain show identical growth kinetics. (*B*) Overexpression of Yno1p substantially slows the growth of BY4741. (*C*) Deletion of the yeast metacaspase, *YCA1*, does not prohibit ROS production in cells overexpressing *YNO1* (*Inset*) but rescues growth kinetics.

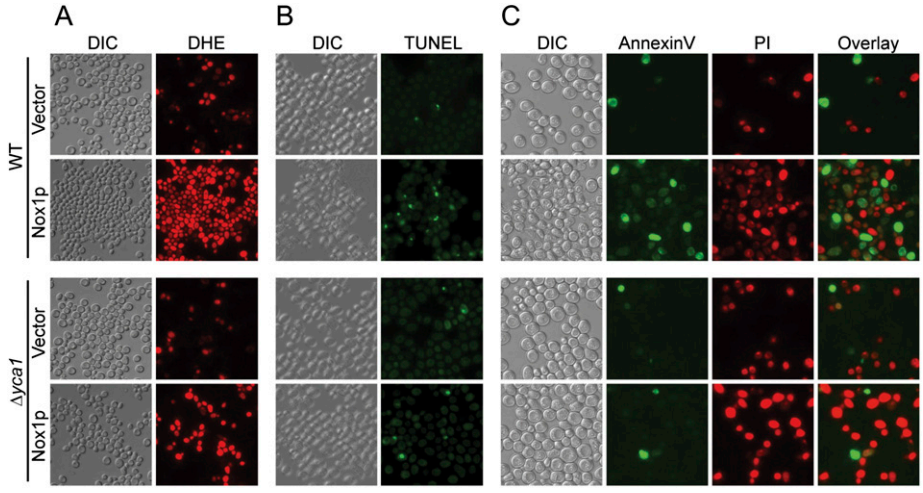

Fig. S11. Examples of the actual fluorescence microscopic determinations of DHE (*A*), TUNEL (*B*), Annexin V, and propidium iodide (PI) (*C*) in four strains (BY4741 pYES2, BY4741 pYES2-*YNO1*, yca1Δ pYES2, and yca1Δ pYES2-*YNO1*). Note that cells staining positively with AnnexinV as well as with PI (late apoptotic) occurred infrequently, but necrotic cells (PI^+) were frequent. Apoptotic markers were prominent in the WT strain overexpressing Yno1, but nearly absent in a strain deleted for YCA1, whereas ROS levels were high in both strains.

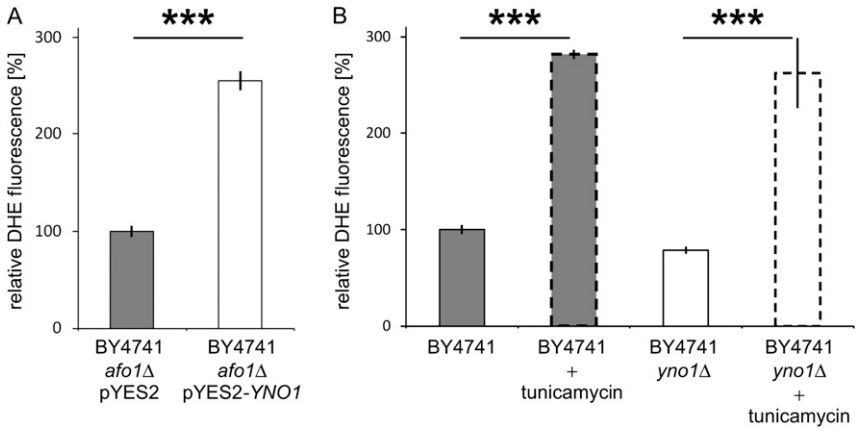

Fig. S12. (*A*) ROS production through *YNO1* overexpression occurred in the *afo1Δ* strain in the same amount as in the control, showing that ROS production through Yno1 is independent of the mitochondrial respiratory chain. (*B*) ROS determinations in BY4741 and *yno1Δ* strains in the presence and absence of tunicamycin (which induces ER stress concomitant with a high level of ROS (1). The fact that tunicamycin induces the same high level of ROS also in an *yno1Δ* strain shows that ER stress is independent of Yno1.

1. Hauptmann P, et al. (2006) Defects in N-glycosylation induce apoptosis in yeast. *Mol Microbiol* 59:765–778.

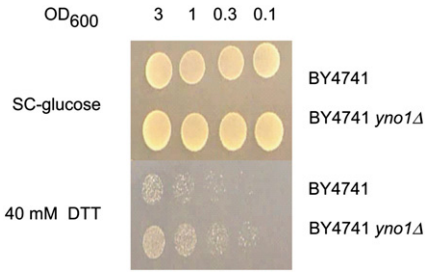

Fig. S13. To test the possible involvement of YNO1 in counteracting reductive stress, wild-type cells and *yno1Δ* cells were spotted on plates containing 40 mM DTT. On these plates, both strains showed similar growth, showing that the deletion of *YNO1* cannot increase reductive stress, which acts primarily through protein aggregation in the ER (1).

1. Trotter EW, Grant CM (2002) Thioredoxins are required for protection against a reductive stress in the yeast Saccharomyces cerevisiae. *Mol Microbiol* 46:869–878.

Table S1. Mean peak intensities (areas under the peaks marked with arrows) and SDs of the superoxide-specific ESR peaks in the two spectra shown in Fig. 2*B*

	BY4741 pYES2	BY4741 pYES2-*YNO1*
Mean	23510.33	79517.67
SD	4626.44	8685.24
SEM	2671.08	5014.42

Three biological replicas each; arbitrary units.